

A CONSTANT MOLECULAR GAS DEPLETION TIME IN NEARBY DISK GALAXIES

F. BIGIEL¹, A.K. LEROY^{2,10}, F. WALTER³, E. BRINKS⁴, W.J.G. DE BLOK⁵, C. KRAMER⁶, H.W. RIX³, A. SCHRUBA³,
K.-F. SCHUSTER⁷, A. USERO⁸, H.W. WIESEMAYER⁹

Accepted for Publication in ApJL

ABSTRACT

We combine new sensitive, wide-field CO data from the HERACLES survey with ultraviolet and infrared data from GALEX and *Spitzer* to compare the surface densities of H₂, Σ_{H_2} , and the recent star formation rate, Σ_{SFR} , over many thousands of positions in 30 nearby disk galaxies. We more than quadruple the size of the galaxy sample compared to previous work and include targets with a wide range of galaxy properties. Even though the disk galaxies in this study span a wide range of properties, we find a strong, and approximately linear correlation between Σ_{SFR} and Σ_{H_2} at our common resolution of 1 kpc. This implies a roughly constant median H₂ consumption time, $\tau_{\text{Dep}}^{\text{H}_2} = \Sigma_{\text{H}_2}/\Sigma_{\text{SFR}}$, of ~ 2.35 Gyr (including heavy elements) across our sample. At 1 kpc resolution, there is only a weak correlation between Σ_{H_2} and $\tau_{\text{Dep}}^{\text{H}_2}$ over the range $\Sigma_{\text{H}_2} \approx 5\text{--}100 \text{ M}_{\odot} \text{ pc}^{-2}$, which is probed by our data. We compile a broad set of literature measurements that have been obtained using a variety of star formation tracers, sampling schemes and physical scales and show that overall, these data yield almost exactly the same results, although with more scatter. We interpret these results as strong, albeit indirect evidence that star formation proceeds in a uniform way in giant molecular clouds in the disks of spiral galaxies.

Subject headings: galaxies: evolution — galaxies: ISM — radio lines: galaxies — stars: formation

1. INTRODUCTION

Giant molecular clouds (GMCs) are the sites of star formation in the Milky Way (e.g., Blitz 1993). Therefore, it is not surprising that a strong correlation is observed between tracers of molecular gas and recent star formation (e.g., Rownd & Young 1999; Wong & Blitz 2002; Leroy et al. 2008; Bigiel et al. 2008), while the correlation between atomic gas and recent star formation is found to be weak or absent within galaxies (e.g., Kennicutt et al. 2007; Bigiel et al. 2008). The details of this correlation have important implications. Its evolution over cosmic time informs our understanding of galaxy assembly (Daddi et al. 2010; Genzel et al. 2010). The finding of short molecular gas consumption times compared to galaxy lifetimes highlights the importance of fueling the inner disks of galaxies. The relatively low efficiency of star formation per dynamical time requires that the star formation process be more complex than simple gravitational collapse (e.g., McKee & Ostriker 2007). Fi-

nally, the relationship between star formation and molecular gas is an important input and benchmark for models attempting to reproduce today's galaxies or galaxy populations.

The importance of this topic has led to several studies of the relationship between surface densities of H₂ and the star formation rate. Many of these focus on single galaxies (e.g., Heyer et al. 2004; Kennicutt et al. 2007; Schuster et al. 2007; Blanc et al. 2009; Verley et al. 2010; Rahman et al. 2010) or a small sample (e.g., Wong & Blitz 2002; Leroy et al. 2008; Bigiel et al. 2008; Wilson et al. 2009; Warren et al. 2010). Restricted by the availability of sensitive and wide-field molecular gas maps, studies of large sets of galaxies (e.g., Young et al. 1996; Kennicutt 1998; Rownd & Young 1999; Murgia et al. 2002; Leroy et al. 2005) mostly used integrated measurements or a few pointings per galaxy. To date, no homogeneous analysis of the correlation between the star formation rate and H₂ surface densities in a large set of nearby galaxies at good spatial resolution exists.

In this letter we take this next logical step, comparing molecular gas — traced by CO emission — to recent star formation — traced by ultraviolet and infrared emission — at 1 kpc resolution across a large sample of 30 nearby galaxies. This sample is significantly larger and more diverse than that of Bigiel et al. (2008, hereafter B08). From 2007-2010, the HERA CO-Line Extragalactic Survey (HERACLES, first maps are presented in Leroy et al. 2009) collaboration used the IRAM 30-m telescope¹¹ to construct maps of CO $J = 2 \rightarrow 1$ emission from 48 nearby galaxies. Because the targets overlap surveys by *Spitzer* (mostly SINGS, Kennicutt et al.

¹ Department of Astronomy, Radio Astronomy Laboratory, University of California, Berkeley, CA 94720, USA; bigiel@astro.berkeley.edu

² National Radio Astronomy Observatory, 520 Edgemont Road, Charlottesville, VA 22903, USA

³ Max-Planck-Institut für Astronomie, Königstuhl 17, 69117 Heidelberg, Germany

⁴ Centre for Astrophysics Research, University of Hertfordshire, Hatfield AL10 9AB, UK

⁵ Astrophysics, Cosmology and Gravity Centre, Department of Astronomy, University of Cape Town, Private Bag X3, Rondebosch 7701, South Africa

⁶ IRAM, Avenida Divina Pastora 7, E-18012 Granada, Spain

⁷ IRAM, 300 rue de la Piscine, 38406 St. Martin d'Hères, France

⁸ Observatorio Astronómico Nacional, C/ Alfonso XII, 3, 28014, Madrid, Spain

⁹ Max-Planck-Institut für Radioastronomie, Auf dem Hügel 69, 53121 Bonn, Germany

¹⁰ Hubble Fellow

¹¹ IRAM is supported by CNRS/INSU (France), the MPG (Germany) and the IGN (Spain).

TABLE 1
GALAXY SAMPLE

Galaxy	D [Mpc]	Galaxy	D [Mpc]
NGC 0337 ^d	24.7	NGC 4254 ^d	20.0
NGC 0628 ^{B08}	7.3	NGC 4321	14.3
NGC 0925	9.2	NGC 4536	14.5
NGC 2403	3.2	NGC 4559	7.0
NGC 2841	14.1	NGC 4569 ^d	20.0
NGC 2903	8.9	NGC 4579 ^d	20.6
NGC 2976	3.6	NGC 4625	9.5
NGC 3049	8.9	NGC 4725	9.3
NGC 3184 ^{B08}	11.1	NGC 4736 ^{B08}	4.7
NGC 3198	13.8	NGC 5055 ^{B08}	10.1
NGC 3351	10.1	NGC 5194 ^{B08}	8.0
NGC 3521 ^{B08}	10.7	NGC 5457	7.4
NGC 3627	9.3	NGC 5713 ^d	26.5
NGC 3938	12.2	NGC 6946 ^{B08}	5.9
NGC 4214	2.9	NGC 7331	14.7

^{B08} Target from B08.

^d Too distant to reach 1 kpc resolution, included in the 1 kpc plots at their respective native resolution.

2003) and GALEX (mostly the NGS, Gil de Paz et al. 2007), excellent multiwavelength data are available for most targets.

2. METHOD

We study all galaxies meeting the following criteria: 1) a HERACLES map containing a robust CO $J = 2 \rightarrow 1$ detection, 2) GALEX far UV (FUV) and *Spitzer* infrared data at $24\mu\text{m}$ (IR), and 3) an inclination $\lesssim 75^\circ$. The first condition excludes low mass galaxies without CO detections. The second removes a few targets with poor *Spitzer* $24\mu\text{m}$ data. The third disqualifies a handful of edge-on galaxies. We are left with 30 disk galaxies, listed in Table 1 along with distances adopted from Walter et al. (2008), LEDA, and NED. This sample is more than four times larger than that of B08 and spans a substantial range in metallicities ($8.36 \lesssim z \lesssim 8.93$)¹² and mass ($8.9 \lesssim \log(M_*) \lesssim 11.0$)¹³.

We follow the approach of B08 with only a few modifications. B08 compared the first seven HERACLES maps to FUV, IR, and $\text{H}\alpha$ emission to infer the relationship between the surface density of H_2 , Σ_{H_2} , and the star formation rate surface density, Σ_{SFR} . As in B08, we estimate Σ_{H_2} from HERACLES CO $J = 2 \rightarrow 1$ emission. We assume a Galactic $X_{\text{CO}} = 2 \times 10^{20} \text{ cm}^{-2} (\text{K km s}^{-1})^{-1}$, correct for inclination, include helium in our quoted surface densities (a factor of 1.36, a difference from B08), and adopt a CO line ratio $I(2-1)/I(1-0) = 0.7$ (note that B08 used a ratio of 0.8).

We estimate Σ_{SFR} (inclination corrected) using a combination of FUV emission and $24\mu\text{m}$ emission. FUV emission traces mainly photospheric emission from O and B stars, with a typical age of $\sim 20\text{--}30$ Myr (Leitherer et al. 1999; Salim et al. 2007) but sensitive to populations up to 100 Myr of age. Infrared emis-

sion at $24\mu\text{m}$ comes from dust mainly heated by young stars. This emission correlates closely with other signatures of recent star formation, especially $\text{H}\alpha$ emission, and so has been used to correct optical and UV tracers for the effects of extinction (Calzetti et al. 2007; Kennicutt et al. 2007). Leroy et al. (2008) motivated this FUV–IR combination, showing that it reproduces other estimates of Σ_{SFR} with $\sim 50\%$ accuracy down to $\Sigma_{\text{SFR}} \approx 10^{-3} \text{ M}_\odot \text{ yr}^{-1} \text{ kpc}^{-2}$.

For 24 galaxies, we use FUV maps from the Nearby Galaxy Survey (NGS, Gil de Paz et al. 2007), for five targets from the All-sky Imaging Survey (AIS) and for one galaxy we use a map from the Medium Imaging Survey (MIS). We use maps of IR emission at $24\mu\text{m}$ from the *Spitzer* Infrared Nearby Galaxies Survey (SINGS, Kennicutt et al. 2003) and the Local Volume Legacy Survey (LVL, Dale et al. 2009). Handling of the maps follows B08.

We convolve the IR and FUV maps to the $13''$ (FWHM) resolution of the HERACLES data. Given the wide distance range of our sample, $13''$ resolution corresponds to physical scales from 180 pc to 1.7 kpc. To avoid being influenced by physical resolution, we create a second set of maps at a common physical resolution of 1 kpc (FWHM), appropriate to carry out a uniform analysis. Five galaxies are too distant to reach 1 kpc resolution. We include them in our “kpc” analysis at their native resolution, 1.4 kpc on average (excluding them does not change our conclusions).

The HERACLES maps are masked to include only significant emission (Leroy et al. 2009). The exact completeness of each map in mass surface density depends on the inclination and, for fixed spatial resolution, the distance of the target. A typical noise level is 25 mK per 5.2 km s^{-1} channel at $13''$ resolution. For the most distant, face-on systems this limit is $I_{\text{CO}} > 0.8 \text{ K km s}^{-1}$ or $5 \text{ M}_\odot \text{ pc}^{-2}$ for our adopted X_{CO} and line ratio. Closer or more inclined systems will be complete to lower Σ_{H_2} .

We sample both sets of maps, one at $13''$ and one at 1 kpc resolution, using a hexagonal grid spaced by one half-resolution element. We keep only sampling points inside the B -band 25th magnitude isophotal radius, r_{25} , and where the HERACLES mask includes emission. At $13''$ resolution, this yields Σ_{SFR} and Σ_{H_2} estimates for a total of $\sim 27,000$ points ($\sim 5,000$ independent measurements) in 30 nearby star-forming galaxies. At 1 kpc resolution, this number drops to $\sim 12,000$ (~ 2000 independent) measurements.

3. RESULTS

Figure 1 shows our data in $\Sigma_{\text{SFR}}\text{--}\Sigma_{\text{H}_2}$ space. The upper panels present measurements at a common angular resolution of $13''$, the lower panels show results for a common physical scale of 1 kpc. The left panels show contours indicating the density of data with each galaxy weighted equally. The right panels directly show each data point. Dotted lines in each plot indicate constant molecular gas depletion times, $\tau_{\text{Dep}}^{\text{H}_2} = \Sigma_{\text{H}_2}/\Sigma_{\text{SFR}}$, i.e., fixed ratios of H_2 -to-SFR.

To make the contour plots, we divide the $\Sigma_{\text{SFR}}\text{--}\Sigma_{\text{H}_2}$ space into 0.1 dex-wide cells to grid the data. During gridding, we assign each data point a weight inversely proportional to the number of data points for the galaxy that it was drawn from. This assigns the same total

¹² Metallicities are adopted from Moustakas et al. (2010) where available and supplemented by data from the compilations in Calzetti et al. (2010) and Marble et al. (2010).

¹³ Stellar masses are estimated using the near IR luminosities from Dale et al. (2007, 2009) and the mass-to-light ratio from Leroy et al. (2008).

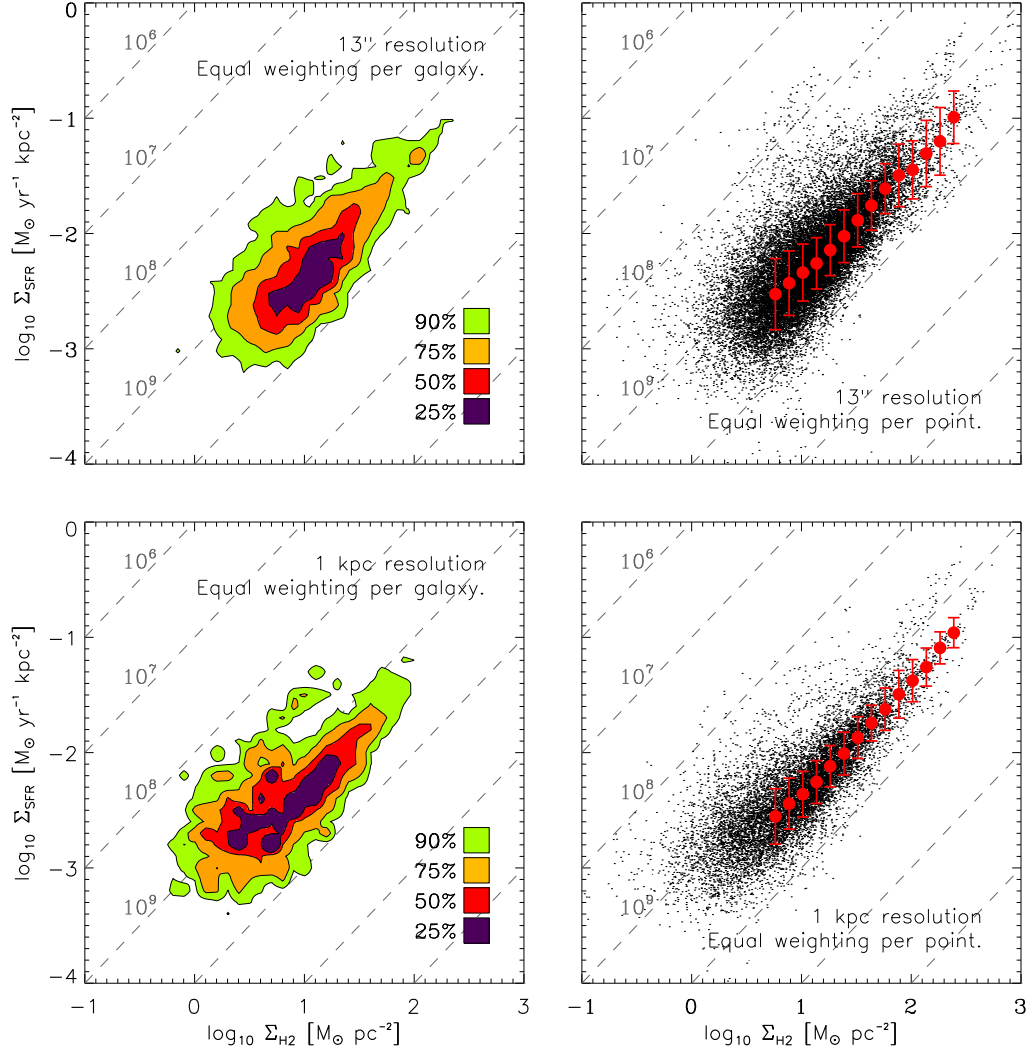


FIG. 1.— Star formation rate surface density, Σ_{SFR} , estimated from FUV+24 μm emission as a function of molecular gas surface density, Σ_{H_2} , estimated from CO $J = 2 \rightarrow 1$ emission for 30 nearby disk galaxies. The left panels show data density with equal weight given to each galaxy. Purple, red, orange, and green contours encompass the densest 25, 50, 75, and 90% of the data. The right panels show each measurement individually as a black dot. The red points indicate running medians in Σ_{SFR} as a function of Σ_{H_2} and the error bars show the 1σ log-scatter in each Σ_{H_2} bin. In both panels, dotted lines indicate fixed H₂ depletion times in yr. Measurements in the top panels are on a common angular scale of 13'', those in the bottom panels are on a common physical scale of 1 kpc. All panels show a strong correlation between Σ_{SFR} and Σ_{H_2} with the majority of data having $\tau_{\text{Dep}}^{\text{H}_2} \sim 2.3 \text{ Gyr}$.

weight to each galaxy, ensuring that a few large galaxies do not drive the overall distribution. Contours indicate the density of sampling points in each cell.

The scatter plots on the right treat all measurements equally, which leads large galaxies to dominate the distribution. While the contour plots treat a galaxy as the fundamental unit, the scatter plots treat each region as a key independent measurement. The red points show a running median in Σ_{SFR} as a function of Σ_{H_2} . Though treating Σ_{H_2} as an independent variable is not rigorous, this binning is a useful way to guide the eye. We only bin where $\Sigma_{\text{H}_2} > 5 \text{ M}_{\odot} \text{ pc}^{-2}$ and we are confident of being complete.

All four plots reveal a strong correlation between Σ_{SFR} and Σ_{H_2} . In this letter we focus our quantitative analysis

on the right hand plots, which weight every measurement equally. The Spearman rank correlation coefficient across all data is $r = 0.8$ at 1 kpc resolution, indicating a strong correlation between Σ_{SFR} and Σ_{H_2} . We find a median H₂ depletion time $\tau_{\text{Dep}}^{\text{H}_2} = 2.35 \text{ Gyr}$ with 1σ scatter 0.24 dex ($\approx 75\%$). The results at fixed 13'' resolution are similar, median $\tau_{\text{Dep}}^{\text{H}_2}$ is $\sim 2.37 \text{ Gyr}$ and $r = 0.7$.

It is common to parameterize relationships between gas and star formation using power law fits. This can be problematic physically, because data from widely varying environments are often not well-described by a single power law (B08, Bigiel et al. 2010b). It is also challenging practically, because of, e.g., issues of completeness and upper limits (see Blanc et al. 2009), zero point uncertainties (compare Rahman et al. 2010) or a correct

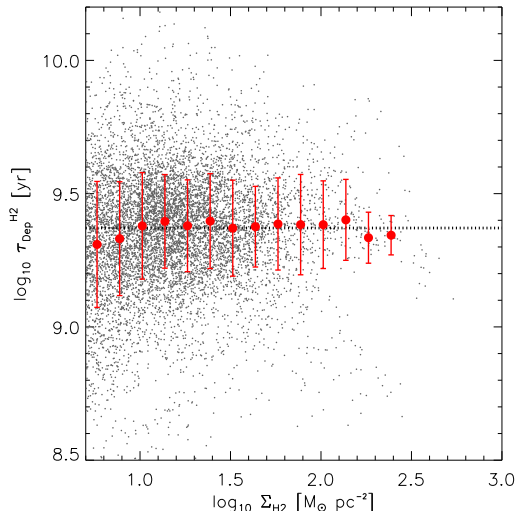


FIG. 2.— $\tau_{\text{Dep}}^{\text{H}_2}$ as a function of Σ_{H_2} . Gray points indicate individual measurements. Red points show the running median. Error bars indicate the 1σ scatter in each bin. The dashed line shows the median $\tau_{\text{Dep}}^{\text{H}_2} \approx 2.35$ Gyr. $\tau_{\text{Dep}}^{\text{H}_2}$ shows little or no systematic variation with H_2 surface density over the range $\Sigma_{\text{H}_2} \sim 5\text{--}100 \text{ M}_{\odot} \text{ pc}^{-2}$.

treatment of the uncertainties associated with physical parameter estimation. Bearing these caveats in mind, a rough parameterization may still be useful to the reader. If we apply a simple linear regression in log space and fit¹⁴ the function $\Sigma_{\text{SFR}} = A \times (\Sigma_{\text{H}_2}/10 \text{ M}_{\odot} \text{ pc}^{-2})^N$ to the binned kpc data (red points in the lower right panel of Figure 1), we find $A \approx 4.4 \times 10^{-3} \text{ M}_{\odot} \text{ yr}^{-1} \text{ kpc}^{-2}$ and $N \approx 1.0$. This is not rigorous: we have treated the observable Σ_{H_2} as an independent variable and we discarded information in the process of binning. However the fit does reasonably bisect the data. We find similar results fitting the individual measurements where we are complete with N varying by ± 0.2 and A varying by $\sim 30\%$, depending mainly on how the fit is constructed.

The results of this fitting can be distilled to what is immediately apparent from the plot: a characteristic $\tau_{\text{Dep}}^{\text{H}_2} \sim 2.3$ Gyr and a power law index close to unity, so that the data extend parallel to the dashed lines of fixed $\tau_{\text{Dep}}^{\text{H}_2}$ in Figure 1. The global index close to unity implies that the ratio of Σ_{H_2} to Σ_{SFR} does not change much as a function of Σ_{H_2} across our data. We quantify this by comparing $\tau_{\text{Dep}}^{\text{H}_2}$ to Σ_{H_2} where we are complete ($\Sigma_{\text{H}_2} > 5 \text{ M}_{\odot} \text{ pc}^{-2}$). Figure 2 plots the individual measurements along with a running median and scatter; both show little or no systematic variation of $\tau_{\text{Dep}}^{\text{H}_2}$ as a function of Σ_{H_2} across the range studied. The rank correlation coefficient relating $\tau_{\text{Dep}}^{\text{H}_2} = \Sigma_{\text{H}_2}/\Sigma_{\text{SFR}}$ to Σ_{H_2} is $r = 0.09 \pm 0.01$ in our kpc data, i.e., the two quantities are only very weakly correlated.

These results extend those found by B08 and Leroy et al. (2008), who also found a roughly constant ratio $\Sigma_{\text{H}_2}/\Sigma_{\text{SFR}}$ for a smaller, less diverse sample. Based on detailed studies of Local Group galaxies (e.g. Blitz et al. 2007; Bolatto et al. 2008; Bigiel et al. 2010a; Fukui & Kawamura 2010), they speculated that the ap-

proximately linear $\Sigma_{\text{SFR}}\text{--}\Sigma_{\text{H}_2}$ relation arises because star formation in disk galaxies takes place in a relatively uniform population of GMCs. Given typical GMC masses of $\sim 10^5\text{--}10^6 \text{ M}_{\odot}$ and sizes of $\sim 50 \text{ pc}$, each of our resolution elements likely averages over at least a few — and often many — GMCs. Thus, in this scenario the relationship between Σ_{H_2} and Σ_{SFR} reduces to a counting exercise: Σ_{H_2} corresponds to a different number of GMCs inside different resolution elements, rather than to changing physical conditions in the molecular gas. This also naturally explains the weak dependence of our results on spatial scale, which merely determines the number of GMCs per resolution element but leaves the average fixed constant $\tau_{\text{Dep}}^{\text{H}_2}$ intact (compare B08 for a detailed discussion).

This scenario does not contradict earlier results finding that $\tau_{\text{Dep}}^{\text{H}_2}$ depends on Σ_{H_2} or M_{H_2} : the strongest measurements of variable $\tau_{\text{Dep}}^{\text{H}_2}$ come from LIRGs and ULIRGs (e.g., Kennicutt 1998; Gao & Solomon 2004), systems with H_2 surface densities significantly exceeding those studied here and where the assumption of a uniform GMC population likely breaks down. Departures are also expected on scales of individual molecular clouds, where only a small fraction of the molecular gas actively forms stars (e.g., Heiderman et al. 2010). We will show in the next section, however, that for normal disk galaxies and on scales greater than a few 100 pc our results agree remarkably well with previous measurements of $\tau_{\text{Dep}}^{\text{H}_2}$.

4. COMPARISON TO LITERATURE DATA

As described in Section 1, many studies have examined the relationship between molecular gas and star formation in nearby disk galaxies over the last decade. The emphasis on power law fits has somewhat obscured the basic question of whether these data fundamentally agree or disagree regarding which part of $\Sigma_{\text{H}_2} - \Sigma_{\text{SFR}}$ space is occupied by local disk galaxies. To address this point, Figure 3 shows our binned data (big points with error bars) along with a wide compilation of recent measurements.

We adjust all literature measurements to share our adopted X_{CO} and stellar IMF (Kroupa), but otherwise leave the data unchanged. These points therefore reflect a wide range of star formation tracers, sampling schemes and physical scales.

We plot averages over whole galaxies as triangles. These include 57 normal spiral galaxies (green) and 15 starburst galaxies (blue) from Kennicutt (1998). Kennicutt (1998) estimates Σ_{SFR} from $\text{H}\alpha$ for normal spirals and IR emission for starbursts. We also show 236 pointings towards spirals from Murgia et al. (2002, purple) and towards 80 small nearby spirals and dwarfs from Leroy et al. (2005, red)¹⁵. Both data sets have $\sim 50''$ resolution, corresponding to $\sim 1\text{--}4 \text{ kpc}$, and use 1.4 GHz radio continuum (RC) emission to estimate Σ_{SFR} .

Filled diamonds indicate radial profile measurements. Data for 7 nearby spirals from Wong & Blitz (2002) are shown in red, those for M51 from Schuster et al.

¹⁵ These studies compile measurements from Young et al. (1995), Taylor et al. (1998), Elfhag et al. (1996), and Böker et al. (2003).

¹⁴ We normalize the fit at $\Sigma_{\text{H}_2} = 10 \text{ M}_{\odot} \text{ pc}^{-2}$ following B08.

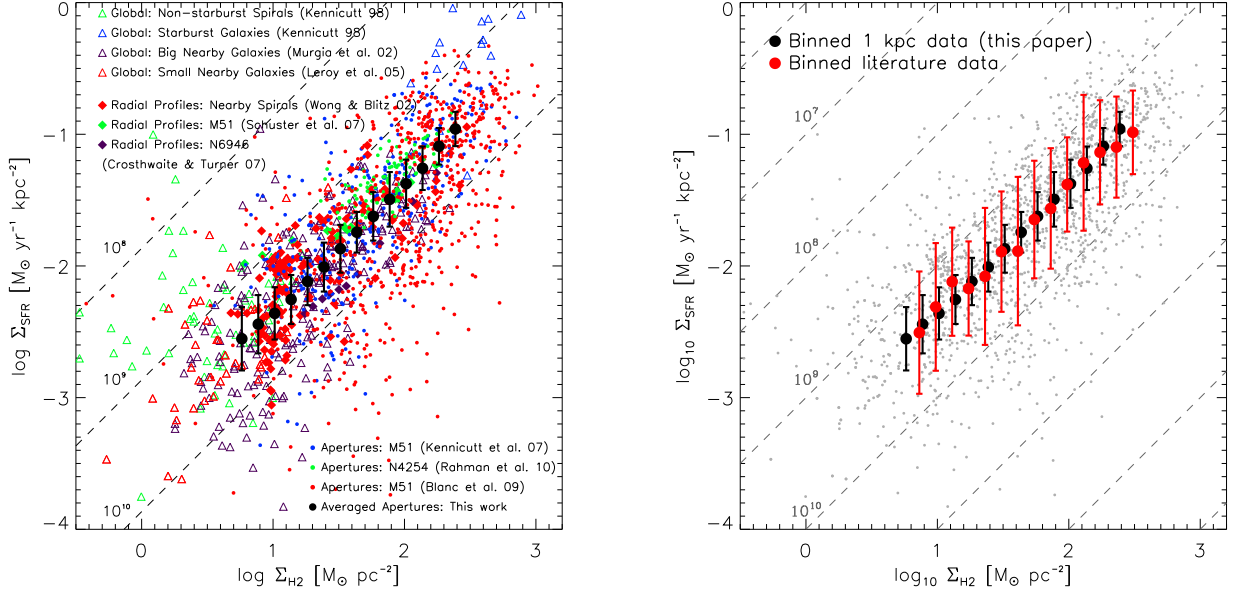


FIG. 3.— Σ_{SFR} versus Σ_{H_2} for a compilation of literature measurements and our binned data. In the left panel we label individual studies, which employ a wide range of star formation tracers, sampling schemes and physical scales. The black points indicate the running medians for our 1 kpc data from Figure 1. In the right panel we treat all literature measurements equally (gray points) and construct a running median (red points) in the same way that we binned our data (black points) in Figure 1. Both panels show excellent agreement between our measurements and the literature data and suggest an emerging consensus on the basic, approximately linear, $\Sigma_{\text{SFR}} - \Sigma_{\text{H}_2}$ relation in nearby disk galaxies.

(2007) in green and those for NGC 6946 from Crosthwaite & Turner (2007) in purple. Wong & Blitz (2002) derive Σ_{SFR} from H α emission, Schuster et al. (2007) from RC emission, and Crosthwaite & Turner (2007) from FIR emission.

Small points represent aperture data. Blue points show 520 pc-sized aperture measurements from Kennicutt et al. (2007) of star forming regions in the spiral arms of NGC 5194 (M51). They infer Σ_{SFR} from a combination of H α and 24 μm emission. Green points show 500 pc apertures from Rahman et al. (2010), who sample mainly the spiral arms of NGC 4254. The points shown here reflect Σ_{SFR} as derived from FUV and 24 μm emission. Red points indicate 170 pc apertures covering the central $4.1 \times 4.1 \text{ kpc}^2$ of NGC 5194 (M51) from Blanc et al. (2009). They infer Σ_{SFR} from extinction corrected H α emission using integral field unit observations. The left panel of Figure 3 labels these various studies and overplots our data.

Figure 3 shows that these measurements sweep out a distinct part of $\Sigma_{\text{SFR}} - \Sigma_{\text{H}_2}$ space. Most data scatter between $\tau_{\text{Dep}}^{\text{H}_2} = 10^9$ and 10^{10} yr and our measurements lie near the center of the distribution. The right panel in Figure 3 shows this most clearly: we take the simplistic approach of treating all of the literature data equally (shown as gray points) and construct the same running median that we use on our own data. The literature average (red points) agrees strikingly well with our measurements (black points). This implies that our results are robust with respect to the choice of tracers or experimental setup. The literature sample as a whole also suggests that $\tau_{\text{Dep}}^{\text{H}_2} \approx 2.3$ Gyr in nearby disks and that $\tau_{\text{Dep}}^{\text{H}_2}$ is a fairly weak function of Σ_{H_2} .

5. SUMMARY

Using new IRAM 30m CO $J = 2 \rightarrow 1$ maps from the HERACLES survey, we determine the relation between H $_2$ surface density, Σ_{H_2} , and SFR surface density, Σ_{SFR} , in 30 nearby disk galaxies. This significantly extends the number of galaxies (by more than a factor of four) and the range of galaxy properties probed compared to Bigiel et al. (2008). We present our main results for a common physical resolution of 1 kpc. We find a remarkably constant molecular gas consumption time $\tau_{\text{Dep}}^{\text{H}_2} \approx 2.35$ Gyr (including helium) with a 1σ scatter of 0.24 dex ($\approx 75\%$) and little dependence of $\tau_{\text{Dep}}^{\text{H}_2}$ on Σ_{H_2} over the range $\Sigma_{\text{H}_2} \sim 5\text{--}100 \text{ M}_\odot \text{ pc}^{-2}$.

This extends and reinforces the conclusions of Bigiel et al. (2008) and Leroy et al. (2008) that the star formation rate per unit H $_2$ in the disks of massive star-forming galaxies is, to first order, constant. We interpret this as strong, yet indirect, evidence that the disks of nearby spiral galaxies are populated by GMCs forming stars in a relatively uniform manner. We caution that these results are specific to disk galaxies and scales on which we average over many GMCs — they may be expected to break down at very high surface densities and on small scales. Taken as a whole, a broad compilation of literature data on disk galaxies from the last decade yields impressively similar results.

We thank the GALEX NGS, SINGS, and LVL teams for making their outstanding datasets available. We thank Karl Gordon for the kernel used on the MIPS 24 μm data and Nurur Rahman for sharing his data. We thank the staff of the IRAM 30m telescope for their assistance carrying out the survey. F.B., A.K.L., and F.W. gratefully acknowledge the Aspen Center for Physics, where part of this work was carried out. Support for

A.K.L. was provided by NASA through Hubble Fellowship grant HST-HF-51258.01-A awarded by the Space Telescope Science Institute, which is operated by the Association of Universities for Research in Astronomy,

Inc., for NASA, under contract NAS 5-26555. The work of W.J.G.d.B. is based upon research supported by the South African Research Chairs Initiative of the Department of Science and Technology and National Research Foundation.

REFERENCES

- Bigiel, F., Leroy, A., Walter, F., Brinks, E., de Blok, W. J. G., Madore, B., & Thornley, M. D. 2008, *AJ*, 136, 2846
- Bigiel, F., Bolatto, A., Leroy, A., Blitz, L., Walter, F., Rosolowsky, E., Lopez, L., & Plambeck, R. 2010a, *ApJ*, 725, 1159
- Bigiel, F., Leroy, A., Walter, F., Blitz, L., Brinks, E., de Blok, W. J. G., & Madore, B. 2010b, *AJ*, 140, 1194
- Blanc, G. A., Heiderman, A., Gebhardt, K., Evans, N. J., & Adams, J. 2009, *ApJ*, 704, 842
- Blitz, L. 1993, in *Protostars and Planets III*, ed. E. H. Levy & J. I. Lunine, 125–161
- Blitz, L., Fukui, Y., Kawamura, A., Leroy, A., Mizuno, N., & Rosolowsky, E. 2007, in *Protostars and Planets V*, ed. B. Reipurth, D. Jewitt, & K. Keil, 81–96
- Böker, T., Lisenfeld, U., & Schinnerer, E. 2003, *A&A*, 406, 87
- Bolatto, A. D., Leroy, A. K., Rosolowsky, E., Walter, F., & Blitz, L. 2008, *ApJ*, 686, 948
- Calzetti, D., et al. 2007, *ApJ*, 666, 870
- Calzetti, D., et al. 2010, *ApJ*, 714, 1256
- Crosthwaite, L. P., & Turner, J. L. 2007, *AJ*, 134, 1827
- Daddi, E., et al. 2010, *ApJ*, 714, L118
- Dale, D. A., et al. 2007, *ApJ*, 655, 863
- Dale, D. A., et al. 2009, *ApJ*, 703, 517
- Elfhag, T., Booth, R. S., Hoeglund, B., Johansson, L. E. B., & Sandqvist, A. 1996, *A&AS*, 115, 439
- Fukui, Y., & Kawamura, A. 2010, *ARA&A*, 48, 547
- Gao, Y., & Solomon, P. M. 2004, *ApJ*, 606, 271
- Genzel, R., et al. 2010, *MNRAS*, 407, 2091
- Gil de Paz, A., et al. 2007, *ApJS*, 173, 185
- Heiderman, A., Evans, N. J., II, Allen, L. E., Huard, T., & Heyer, M. 2010, *ApJ*, 723, 1019
- Heyer, M. H., Corbelli, E., Schneider, S. E., & Young, J. S. 2004, *ApJ*, 602, 723
- Kennicutt, Jr., R. C. 1998, *ApJ*, 498, 541
- Kennicutt, Jr., R. C., et al. 2003, *PASP*, 115, 928
- Kennicutt, Jr., R. C., et al. 2007, *ApJ*, 671, 333
- Leitherer, C., et al. 1999, *ApJS*, 123, 3
- Leroy, A., Bolatto, A. D., Simon, J. D., & Blitz, L. 2005, *ApJ*, 625, 763
- Leroy, A. K., Walter, F., Brinks, E., Bigiel, F., de Blok, W. J. G., Madore, B., & Thornley, M. D. 2008, *AJ*, 136, 2782
- Leroy, A. K., et al. 2009, *ApJ*, 702, 352
- Marble, A. R., et al. 2010, *ApJ*, 715, 506
- McKee, C. F., & Ostriker, E. C. 2007, *ARA&A*, 45, 565
- Moustakas, J., Kennicutt, R. C., Jr., Tremonti, C. A., Dale, D. A., Smith, J.-D. T., & Calzetti, D. 2010, *ApJS*, 190, 233
- Murgia, M., Crapsi, A., Moscadelli, L., & Gregorini, L. 2002, *A&A*, 385, 412
- Rahman, N., et al. 2010, *ApJ*, in press, arXiv:1009.3272
- Rownd, B. K., & Young, J. S. 1999, *AJ*, 118, 670
- Salim, S., et al. 2007, *ApJS*, 173, 267
- Schuster, K. F., Kramer, C., Hitschfeld, M., García-Burillo, S., & Mookerjee, B. 2007, *A&A*, 461, 143
- Taylor, C. L., Kobulnicky, H. A., & Skillman, E. D. 1998, *AJ*, 116, 2746
- Verley, S., Corbelli, E., Giovanardi, C., & Hunt, L. K. 2010, *A&A*, 510, A64
- Walter, F., Brinks, E., de Blok, W. J. G., Bigiel, F., Kennicutt, R. C., Thornley, M. D., & Leroy, A. 2008, *AJ*, 136, 2563
- Warren, B. E., et al. 2010, *ApJ*, 714, 571
- Wilson, C. D., et al. 2009, *ApJ*, 693, 1736
- Wong, T., & Blitz, L. 2002, *ApJ*, 569, 157
- Young, J. S., et al. 1995, *ApJS*, 98, 219
- Young, J. S., Allen, L., Kenney, J. D. P., Lesser, A., & Rownd, B. 1996, *AJ*, 112, 1903